Intensity ratio among Ne-like FeXVII n=3-2 transitions

Shigeru MORITA[1,2], Xianli HUANG[2], Tetsutarou OISHI[1,2], Izumi MURAKAMI[1,2], Hongming ZHANG[2] and Motoshi GOTO[1,2]

[1] National Institute for Fusion Science, Toki, Gifu 509-5292, Japan

[2] Department of Fusion Science, SOKENDAI (The Graduate University for Advanced Studies), Toki, Gifu 509-5292, Japan

Radial profiles of FeXVII 3s-2p and 3d-2p transitions emitted in wavelength range of 15-17Å have been observed in Large Helical Device (LHD). The Chord-integrated radial profiles are converted into radial emissivity profile by means of Abel inversion. The emissivity ratios among FeXVII n=3-2 transitions calculated from the radial emissivity profile are compared with calculation based on a collisional-radiative (CR) model developed for Fe ions. The result reasonably confirms the effect of electron temperature and density on the emissivity ratios. However, the emissivity of 3C ($2p^5 3d\ ^1P_1 \rightarrow 2p^6$) transition is obviously lower than the prediction from the CR model. This discrepancy is consistent with measurements in the solar corona and other laboratory plasmas.

Keywords: Ne-like iron, FeXVII, Intensity ratio, EUV spectroscopy

I. Introduction

Ne-like ion in the ionization balance of iron element is a dominant ionization state existing over a broad electron temperature range in both the cosmic and laboratory plasmas due to its closed L shell atomic configuration. Therefore, the 3s-2p and 3d-2p transitions of Ne-like iron (Fe^{16+}) at wavelength range of 15-17Å, which are prominent for diagnosing high-temperature plasmas, have been extensively studied in both the astrophysical and laboratory plasma studies, including the fusion plasma research [1-7]. A collisional-radiative (CR) model theoretically predicts that the intensities of FeXVII lines at 17.097Å, 17.054Å, and 16.777Å are dependent on not only electron temperature but also electron density. Therefore, the FeXVII lines with transitions of n=3 to n=2 called Lα transition are very useful for measurements of electron temperature [8], electron density [5] and ion abundance [1]. In addition to such diagnostics, the Lα transitions can be applied to the impurity transport study in fusion plasma research because their intensities are considerably strong [9]. In spite of this importance, however, observed intensities of a few FeXVII lines have not been well interpreted with the C-R modeling. For example, the observed overall intensity of 3s-2p transitions is larger than the theoretically predicted one when it is compared with the intensity of 3d-2p transitions [10]. A significant discrepancy between the observation and calculation exists in the intensity of the 3d-2p transition at 15.015Å [11]. Therefore, further investigation is necessary to explore the underlying physical processes related to the Ne-like FeXVII intensities.

II. Spectra and radial profiles of Ne-like FeXVII n=3-2 transitions

In Large Helical Device (LHD), the Fe n=3-2 Lα transition array composed of ionization stages of Ne-like Fe^{16+} to Li-like Fe^{23+} ions have been observed at wavelength interval of 10-20Å. Figure 1 shows typical spectra of Fe Lα array in different electron temperatures. Several FeXVII lines have been identified from the spectra as:

3C: 15.015 Å ($2p^5 3d\ ^1P_1 \rightarrow 2p^6\ ^1S_0$),
3D: 15.262Å ($2p^5 3d\ ^3D_1 \rightarrow 2p^6\ ^1S_0$),
3E: 15.450Å ($2p^5 3d\ ^3P_1 \rightarrow 2p^6\ ^1S_0$),
3F: 16.777 Å ($2p^5 3s\ ^3P_1 \rightarrow 2p^6\ ^1S_0$),

3G: 17.054 Å ($2p^5 3s\ ^1P_1 \rightarrow 2p^6\ ^1S_0$) and
M2: 17.097 Å ($2p^5 3s\ ^3P_2 \rightarrow 2p^6\ ^1S_0$).

The 3G line is blended into the M2 line due to a limited spectral resolving power. The 3E line is usually weak for the observation. The 3G+M2 and 3C lines show the strongest intensity in the Fe Lα transition array. It is very clear that the Ne-like FeXVII is entirely dominant in the Fe n=3-2 transition array when the electron temperature is low (see Fig.1 (a)), whereas the Fe Lα lines from higher ionization stages, e,g. FeXXI, are gradually strong when the electron temperature increases (see Figs.1 (b) and (c)).

The vertical profiles of FeXVII lines have been measured with a flat-field space-resolved extreme ultraviolet (EUV) spectrometer working in wavelength range of 10-130Å on LHD [12]. The EUV spectrometer consisting of a slit, a holographic grating and a charged coupled device (CCD) detector is installed on a midplane spectrometer port at the backside of a rectangular vacuum extension chamber connected to a midplane LHD port. The observation chords of the spectrometer passing through a horizontal slit for spatial resolution placed between the grating and the entrance slit have a small upper elevation angle to observe a vertical profile at upper half (Z=0-50 cm) of horizontally elongated plasma cross section. In the present study the vertical profile is observed with a spatial resolution of 3cm and the data are taken with a temporal resolution of 200ms. The resolving power ($\equiv\lambda/\Delta\lambda$) at λ=17Å is 400 during the line identification and 80 during the profile measurement. Figure 2 (a) shows the vertical profiles of line intensity integrated along the observation chords against different FeXVII transitions of 3C, 3D, 3F and 3G+M2.

The radial emissivity profiles shown in Fig.2 (b) are derived from the vertical profiles in Fig.2 (a) based on an Abel inversion technique. The magnetic flux surface structure in LHD plasmas is calculated with a variation moments equilibrium code (VMEC) [13]. Then, the integral lengths of emissivity at all magnetic surfaces are evaluated with finite-β value along the observation chords of the spectrometer. Here, it should be pointed out that the magnetic flux surfaces are also assumed outside the last close flux surface (LCFS) by extrapolating the magnetic surface contour. Although the assumption may cause certain uncertainty, it does not strongly affect the emissivity peak inside the LCFS because the emissivity outside the LCFS is usually weak.

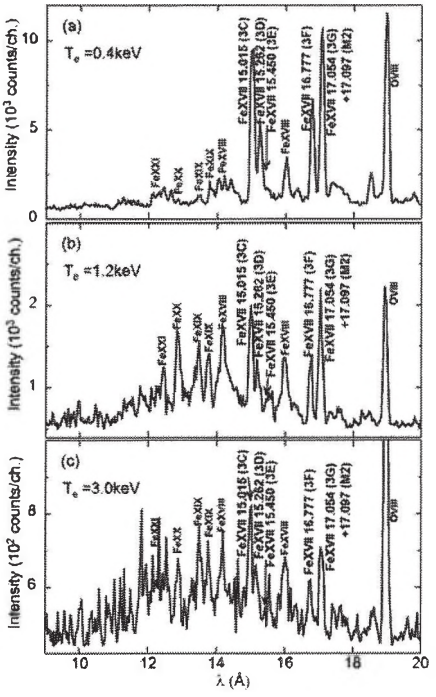

Fig.1 EUV spectra of Fe n=3-2 transitions in discharges with different electron temperatures of (a) 0.4 keV, (b) 1.2 keV and (c) 3.0 keV.

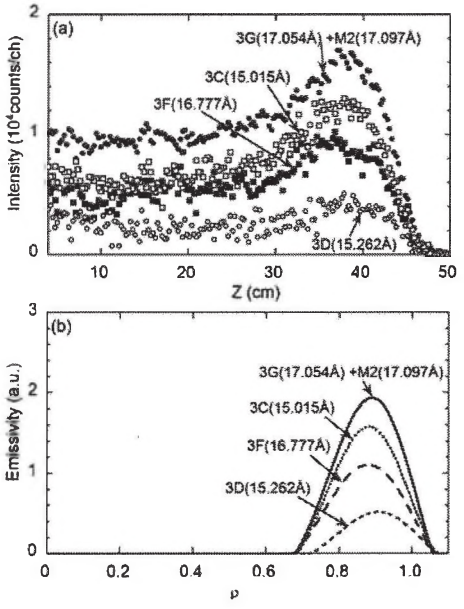

Fig.2 (a) Vertical profiles of chord-integrated intensity and (b) emissivity profiles as a function of normalized radius in Ne-like ArVII n=3-2 transitions.

III. Collisional-radiative (CR) model for iron

A CR model is developed for Fe ions including the fine-structure levels with the principal quantum number up to n = 5 [14, 15]. Assuming a quasi-steady state, the CR model includes all relevant atomic processes necessary for determining the level population. Most of atomic data are calculated with HULLAC code [16]. Although the population density of an excited level contains both the ionizing and recombining plasma components and a recombination component, the ionizing plasma component is the dominant process because the plasma discharge is stable and the recombining process is only dominant in the plasma termination phase.

The intensity coefficients of Fe XVII transitions are calculated with the CR model. The result is shown in Fig.3. The population in the upper levels of 3d-2p transitions (3C, 3D and 3E) is mainly determined by the collisional excitation from the ground level, whereas the upper levels of 3s-2p transitions (3F, 3G and M2) are dominantly populated by the cascade from higher levels [17]. The population redistribution through collision appears in the 3s-2p transitions when the electron density increases above 10^{13} cm^{-3} [5]. As a result, the intensity of 3G and 3F lines increases with density, while the M2 intensity decreases with density because the M2 line is a forbidden transition. The M2 intensity is then more sensitive to the density.

IV. Analysis of emissivity ratio among FeXVII n=3-2 transitions

The emissivity of 3C, 3D and 3F transitions is analyzed by taking the ratio against the 3G+M2 transition. The ratio is evaluated at the peak position of emissivity profiles in electron density range of n_e = 1-5×$10^{13}$$cm^{-3}$. The emissivity ratios analyzed here is shown in Fig.4 as a function of electron temperature, T_e. The result from theoretical calculation with the CR model is also shown in Fig. 4. The temperature and density profiles measured by Thomson scattering diagnostic is used in the analysis.

In the CR model calculation it is predicted that the emissivity ratios of 3D and 3F to 3G+M2 transitions, i.e., $\varepsilon_{3D}/\varepsilon_{(3G+M2)}$ and $\varepsilon_{3F}/\varepsilon_{(3G+M2)}$, are not sensitive to the electron temperature. The measurement plotted in Fig.4 also indicates a weak dependence on T_e and show a good agreement with the theoretical prediction. On the other hand, it is also predicted that the emissivity ratio, $\varepsilon_{3C}/\varepsilon_{(3G+M2)}$, increases with T_e. The ratio is then carefully investigated as plotted in Fig.3. It is found that the measured ratio is smaller than the theoretical calculation by 25-40%. Since the ratios of $\varepsilon_{3D}/\varepsilon_{(3G+M2)}$ and $\varepsilon_{3F}/\varepsilon_{(3G+M2)}$ are in good agreement between the measurement and calculation, the discrepancy in the ratio of $\varepsilon_{3C}/\varepsilon_{(3G+M2)}$ should be attributed to an overestimate of the 3C emissivity.

The discrepancy related to the 3C emissivity has been also studied in laboratory and astrophysical plasmas based on the analysis of the ratio, $R \equiv \varepsilon_{3C}/\varepsilon_{3D}$. The ratio of R in the present

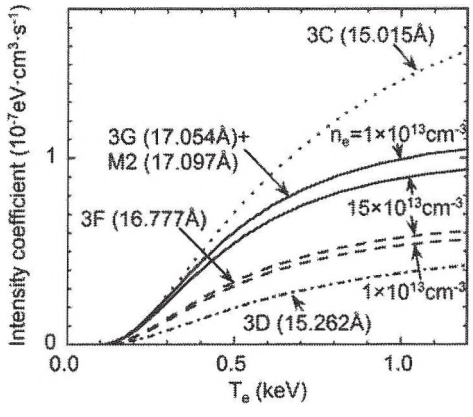

Fig.3 Intensity coefficients of FeXVII n=3-2 transitions as a function of electron temperature calculated with CR model.

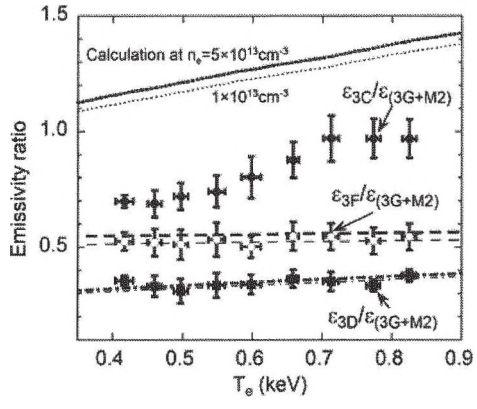

Fig.4 Emissivity ratios of FeXVII transitions as a function of electron temperature (circles and squares: measurement, lines: CR model calculation).

study ranges from 2.0 to 2.9 as T_e increases from 0.4 keV to 0.8 keV. The value is obviously lower than the predicted range of R=3.6-3.7. The present result is entirely consistent with the results from the solar corona [18], Princeton Large Torus (PLT) tokamak [6] and electron beam ion traps (EBITs) [3,19]. It also reveals that the discrepancy is not originated in certain effects related to chord-integrated information. Although there is no atomic theory explaining the discrepancy at present, a result from EBIT at Lawrence Livermore National Laboratory (LLNL) suggests that the excitation cross section of the 3C transition in the theoretical calculation is obviously underestimated, while the cross section of the 3D transition is in a good agreement with theory [20]. A recent study on the oscillator strength of 3C/3D suggests that the discrepancy is caused by the accuracy in atomic wave functions [21]. In order to obtain more accurate theoretical ratio, which should be close to the experimental value, further improvement is necessary for theoretical modeling including more complete treatment on spin-orbit interaction.

In addition to the T_e dependence of the ratio, the density effect on the ratio of $\varepsilon_{3F}/\varepsilon_{(3G+M2)}$ has been also examined. The density effect is studied by analyzing two discharges with distinctly different densities. The result is shown in Fig. 5. The shot numbers of #119551 and #118639 indicate a high-density discharge with flat T_e and centrally peaked n_e profiles and a low-density discharge with centrally peaked T_e and flat n_e profiles, respectively (see Figs.5 (b) and (c)). The emissivity ratio analyzed from the profiles is plotted in Fig.5 (a) with the result from CR model calculation. Due to the data scattering in the vicinity of plasma edge and the uncertainty in the Abel inversion near the plasma center, the emissivity ratio profile is expressed in a limited range of normalized radius from ρ=0.2 to 0.8.

The emissivity ratio at high density (#119551) is evidently larger than that at low density (#118639). Since the temperature of two discharge is almost identical in the region of $0.6<\rho<0.8$, the difference in the emissivity ratio between two discharges is certainly attributed to the density effect. These different values of measured ratio also show an excellent agreement with the CR model calculation. Furthermore, it is noticed that the ratio of #119551 increases with the density as a function of ρ because the temperature radially keeps constant, while the ratio of #118639 increases with the temperature as a function of ρ.

The space-resolved spectra from discharges similar to shot #119551 have been analyzed to study the density dependence of $\varepsilon_{3F}/\varepsilon_{(3G+M2)}$. Figure 6 shows the measured ratio as a function of

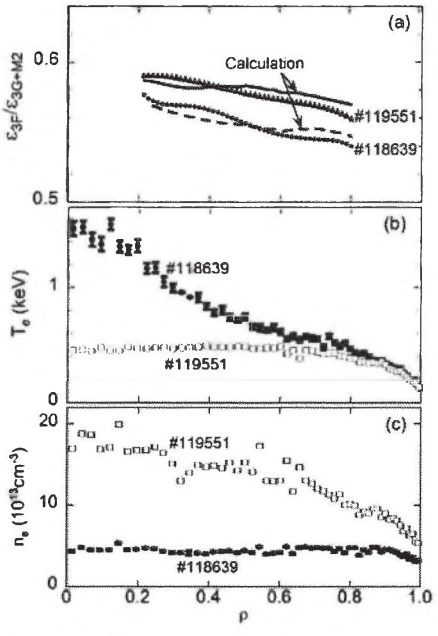

Fig.5 (a) Emissivity ratio profiles of $\varepsilon_{3F}/\varepsilon_{(3G+M2)}$ in two discharges at different densities (triangles and circles: measurement, lines: CR model calculation) (b) electron temperature profiles and (c) electron density profiles.

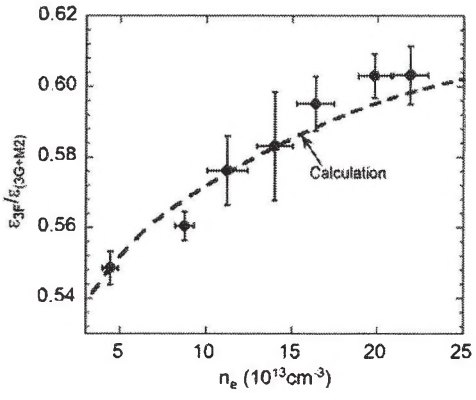

Fig.6 Emissivity ratio of $\varepsilon_{3F}/\varepsilon_{(3G+M2)}$ as a function of electron density (closed circles: measurement, dashed line: CR model calculation).

electron density. The result from CR model calculation is also plotted by dashed line. In the analysis, the electron temperature is fixed at 0.5 keV where the Ne-like iron is usually located. The ratios obtained here agree well with the theoretical calculation in density range of n_e=4-22×10^{13} cm^{-3}, while the relatively large error bars are due to a low signal-to-noise ratio in the measured signal. As a result, the density effect on the FeXVII emissivity ratio is clearly confirmed through the present study.

V. Summary

Ne-like FeXVII n=3-2 Lα transitions denoted with labels of 3C, 3D, 3E, 3F, 3G and M2 have been observed with radial intensity profiles from LHD plasmas. Radial emissivity profiles of the FeXVII transitions are calculated from the intensity profiles by means of Abel inversion and the emissivity ratios among the FeXVII transitions are analyzed. A CR model specially developed for Fe ions is applied for analyzing the data. Although the emissivity ratios of $\varepsilon_{3D}/\varepsilon_{(3G+M2)}$ and $\varepsilon_{3F}/\varepsilon_{(3G+M2)}$ well agree with the CR model calculations, the emissivity ratio of $\varepsilon_{3C}/\varepsilon_{(3G+M2)}$ shows a clear discrepancy by 25%-40%. The result indicates that the discrepancy is not caused by the chord-integrated effect in the measured intensity. The density effect on the emissivity ratio of $\varepsilon_{3F}/\varepsilon_{(3G+M2)}$ is also examined. The result experimentally verifies that the ratio is also sensitive to the electron density as well as to the electron temperature.

Acknowledgements

The authors would like to thank all the members of the LHD team for their cooperation. This work was partially carried out under the LHD project financial support (NIFS13ULPP010) and supported by the JSPS-NRF-NSFC A3 Foresight Program in the field of Plasma Physics (NSFC: No.11261140328, NRF: 2012K2A2A6000443).

References

[1] K. Waljeski, D. Moses, K.P. Dere, J. Saba, D. Web, and D. Zarro, Astrophys. J, **429**, 909 (1994).
[2] S.M. Kahn, F.D. Seward, and T. Chlebowski, Astrophys. J, **283**, 286 (1984).
[3] G. V. Brown *et al.*, Astrophys. J, **502**, 1015 (1998).
[4] K. J. H. Phillips *et al.*, Astron. Astrophys. **324**, 381 (1997).
[5] M. Klapisch *et al.*, Phys. Lett. A, **69**, 34 (1978) .
[6] P. Beiersdorfer, S. von Goeler, M. Bitter, and D.B. Thorn, Phys. Rev. A, 64, 032705 (2001).
[7] P. Beiersdorfer, M. Bitter, S. von Goeler, and K. W. Hill, Astrophys. J, **610**, 616 (2004).
[8] J. C. Raymond, and B.W. Smith, Astrophys. J, **306**, 762 (1986).
[9] P. Beiersdorfer *et al.*, Rev. Sci. Instrum., **60**, 895 (1989).
[10] U. Feldman, Comments At. Mol. Phys., 31, 11 (1995).
[11] J. L. Saba, J. Y. Schmelz, A. K. Bhatia, and K. T. Strong, Astrophys. J, **510**, 1064 (1999).
[12] X. L. Huang, S. Morita, T. Oishi et al., to be published in Rev. Sci. Instrum.
[13] S. P. Hirshman, *et al.*, Comput. Phys. Commun. 43, 143 (1986).
[14] N. Yamamoto *et al.*, Astrophys. J. **689**, 646 (2008).
[15] I. Murakami *et al.*, Plasma and Fusion Research, **5**, S2021 (2010).
[16] A. Bar-Shalom, M. Klapisch, and J. Oreg, J. Quant. Spectrosc. Radiat. Trans., **71**, 179 (2001).
[17] B.W. Smith, J. C. Raymond, J. B. Mann, and R. D. Cowan, Astrophys. J, **298**, 898 (1985).
[18] A. K. Bhatia and J. L. R. Saba, Astrophys. J. 563,434 (2001).
[19] J. M. Laming *et al.*, Astrophys. J., **545**, L161 (2000).
[20] G. V. Brown, Can. J. Phys. **86**,199 (2008).
[21] S. Bernitt, *et al.*, Nature, **492**, 225 (2012).